IJMS
Vol 49, No 2, February 2024

Original Article

Chlorogenic Acid Inhibits Progressive Pulmonary Fibrosis in a Diabetic Rat Model

Sagita Mega Sekar Kencana[1,2], MD; Nur Arfian[1], MD, PhD; Ratih Yuniartha[1], MD, PhD; Ramadhea Laila Afifa An-Nur Willya Saputri[1,2], MD; Fauziyatul Munawaroh[2,3], MD; Dwi Cahyani Ratna Sari[1], MD

[1]Department of Anatomy, School of Medicine, Public Health, and Nursing, Universitas Gadjah Mada, Yogyakarta, Indonesia;
[2]Master Program in Biomedical Sciences, Faculty of Medicine, Public Health, and Nursing, Universitas Gadjah Mada, Yogyakarta, Indonesia;
[3]Faculty of Medicine, IPB University, Bogor, West Java, Indonesia

Correspondence:
Nur Arfian, MD, PhD;
Jalan Farmako, Sekip Utara, Postal code: 55281, Yogyakarta, Indonesia
Email: nur_arfian@ugm.ac.id
Received: 22 October 2022
Revised: 02 January 2023
Accepted: 04 March 2023

Abstract

Background: Chlorogenic acid (CGA) is known to have antifibrotic and hypoglycemic effects and may play a role in preventing diabetes-induced pulmonary fibrosis. This study aimed to determine the effect and optimum dose of CGA on diabetes-induced pulmonary fibrosis.

Methods: Thirty Wistar rats (two-month-old, 150-200 grams) were randomly divided into six groups, namely control, six weeks diabetes mellitus (DM1), eight weeks DM (DM2), and three DM2 groups (CGA1, CGA2, and CGA3) who received CGA doses of 12.5, 25, and 50 mg/Kg BW, respectively. After six weeks, CGA was administered intraperitoneally for 14 consecutive days. Lung tissues were taken for TGF-β1, CTGF, SMAD7, Collagen-1, and α-SMA mRNA expression analysis and paraffin embedding. Data were analyzed using one-way ANOVA and the Kruskal-Wallis test. $P<0.05$ was considered statistically significant.

Results: TGF-β1 expression in the CGA1 group (1.01±0.10) was lower than the DM1 (1.33±0.25, $P=0.05$) and DM2 (1.33±0.20, $P=0.021$) groups. α-SMA expression in the CGA1 group (median 0.60, IQR: 0.34-0.64) was lower than the DM1 (median 0.44, IQR: 0.42-0.80) and DM2 (median 0.76, IQR: 0.66-1.10) groups. Collagen-1 expression in the CGA1 group (0.75±0.13) was lower than the DM1 ($P=0.24$) and DM2 ($P=0.26$) groups, but not statistically significant. CTGF expression in CGA groups was lower than the DM groups ($P=0.088$), but not statistically significant. There was an increase in SMAD7 expression in CGA groups ($P=0.286$). Histological analysis showed fibrosis improvement in the CGA1 group compared to the DM groups.

Conclusion: CGA (12.5 mg/Kg BW) inhibited the expression of profibrotic factors and increased antifibrotic factors in DM-induced rats.

Please cite this article as: Kencana SMS, Arfian N, Yuniartha R, Saputri RLAANW, Munawaroh F, Sari DCR. Chlorogenic Acid Inhibits Progressive Pulmonary Fibrosis in a Diabetic Rat Model. Iran J Med Sci. 2024;49(2):110-120. doi: 10.30476/IJMS.2023.96535.2868.

Keywords ● Pulmonary fibrosis ● Diabetes mellitus ● Chlorogenic acid

What's Known

- Chlorogenic acid (CGA) has the potential to prevent bleomycin-induced pulmonary fibrosis by inhibiting endoplasmic reticulum stress.
- CGA has hypoglycemic and antifibrotic effects on diabetic cardiomyopathy.

What's New

- Low-dose CGA inhibits diabetes-induced pulmonary fibrosis by reducing TGF-β1 mRNA expression.
- Hypoglycemic effect of CGA might not be dose-dependent.

Introduction

Diabetes mellitus (DM) is a chronic metabolic condition characterized by high blood glucose levels (BGL), which may lead to multiple organ damage.[1] As a major complication, DM affects the respiratory system, especially the lungs. Recent clinical studies indicated that DM causes chronic progressive diseases such as pulmonary fibrosis; however, the mechanism

involved has not yet been elucidated.[2-4] The disease causes structural damage to the lungs, stiffening of lung tissue, and ultimately loss of lung function.[2, 5] Several studies reported that pulmonary disorder causes loss of elastic recoil in the lungs of patients with type I DM and reduces forced vital capacity, total lung capacity, and carbon monoxide diffusion capacity.[4-7]

It is suggested that lung tissue damage in DM patients is caused by increased reactive oxygen and/or nitrogen species or a decrease in antioxidant capacity. Oxidative stress activates nuclear factor kappa B (NF-κB), which in turn induces transcription of proinflammatory cytokines.[8] Oxidative stress is also associated with activation and production of transforming growth factor-beta 1 (TGF-β1). Activation of TGF-β1 induces fibroblast proliferation, increases the expression of connective tissue growth factor (CTGF), conversion of fibroblasts into myofibroblasts, and accumulation of extracellular matrix. It also causes pulmonary parenchymal fibrosis characterized by the accumulation of type 1 collagen (collagen-1), fibronectin, and alpha-smooth muscle actin (α-SMA).[7-9] Myofibroblasts play an important role in fibrosis by forming fibrotic foci. They are responsible for the synthesis and deposition of the extracellular matrix, as well as changes in contractile properties of lung tissue that lead to changes in tissue structure and subsequent loss of lung function.[10]

There have been various studies on the anti-fibrotic effect of several antidiabetic drugs,[11, 12] but there are no studies on their ability to reduce the occurrence of organ damage. One such drug is metformin, which has shown beneficial effects on lung fibrosis, independent of its hypoglycemic effect.[13] Chlorogenic acid (CGA) is a phenolic compound widely found in some fruits and coffee. CGA is a potent antioxidant, because it has two phenol groups as free radical scavengers.[14] Studies have not only shown the antidiabetic and antilipidemic effects of CGA,[15] but also its anti-fibrotic effect on various organs.[16-18] To the best of our knowledge, to date, no studies have investigated the effect of CGA on diabetes-induced pulmonary fibrosis. The present study, therefore, aimed to determine the effect and optimum dose of CGA on diabetes-induced pulmonary fibrosis.

Materials and Methods

Rat Model of Diabetes

A quasi-experimental study was conducted in 2020 at the Faculty of Medicine, Gadjah Mada University (Yogyakarta, Indonesia). The study was carried out and reported in accordance with the Animal Welfare Guidelines of Gadjah Mada University, the Forum for Ethical Review Committees in the Asian and Western Pacific Region (FERCAP), and Improving the Reporting of Animal Experiments (ARRIVE).[19] In addition, the study was approved by the Ethics Committee of Gadjah Mada University (number: KE/FK/1087/EC/2020).

Thirty male Wistar rats (two months old, 150-200 g) were used in the experiments. The sample size was determined using the Federer formula. The rats were housed under controlled conditions, 12:12 hours light-dark cycle, and access to food and water ad libitum. Based on the type of treatment and time of euthanasia, the animals were randomly divided into six groups (five rats per group), namely control, DM1 (DM for six weeks), DM2 (DM for eight weeks), CGA1 (DM2 group treated with CGA 12.5 mg/Kg body weight [BW]), CGA2 (DM2 group treated with CGA 25 mg/Kg BW), and CGA3 (DM2 group treated with CGA 50 mg/Kg BW).

Diabetes was induced by intraperitoneal injection of a single-dose streptozotocin (Cayman Chemical, Michigan, USA) dissolved in sodium citrate buffer at a dose of 60 mg/Kg BW. BGL was evaluated on day six post-injection to confirm diabetes (pre-CGA). Diabetes was confirmed when BGL was higher than 250 mg/dL. Rats that received the same volume of 0.9% sodium chloride were used as controls and euthanized at week eight. CGA (part number: C3878, Sigma-Aldrich) was dissolved in phosphate-buffered saline (PBS) and intraperitoneally administered at a dose of 12.5 mg/Kg BW (CGA1), 25 mg/Kg BW (CGA2), and 50 mg/Kg BW (CGA3) for 14 consecutive days, starting from week six after the induction of diabetes. The DM2 group also received PBS as a vehicle during the same period.

Prior to euthanasia, the BGL of all rats was assessed for the hypoglycemic effect of CGA (post-CGA). The rats in the DM1 group (after six weeks) and all other groups (after eight weeks) were sacrificed by intramuscular ketamine injection (part number: KTM100, PT. Bernofarm Pharmaceutical, Indonesia) at a dose of 100 mg/Kg BW. The abdomen and thorax were then opened, and the left ventricle was perfused with 0.9% sodium chloride. The lungs were removed and fixed in neutral buffered formalin for paraffin embedding. In addition, 100 mL FavorPrep™ RNA stabilization solution (part number: FARSS 001, Favorgen®, Taiwan) was used for RNA extraction.

RNA Extraction and Reverse Transcriptase Polymerase Chain Reaction (RT-PCR)

RNA from the lung tissues was isolated using

an RNA stabilization solution according to the manufacturer's protocol. RNA concentrations were quantified using a NanoDrop® spectrophotometer. The RNA was synthesized to cDNA using ExcelRT™ Reverse Transcription Kit II, 100 Rxn (part number: RP1400, Smobio Technology, Inc., Taiwan). PCR was performed in 35 cycles at 25 °C for 10 minutes (denaturation), 42 °C for 50 minutes (annealing), and 85 °C for 5 minutes (extension). cDNA samples were then stored at -20 °C.

RT-PCR was performed to amplify the cDNA of TGF-β1, CTGF, collagen-1, α-SMA, and hypoxanthine-guanine phosphoribosyltransferase 1 (HPRT1) as housekeeping genes. The sequence of primers and PCR conditions are presented in table 1. RT-PCR was performed by mixing cDNA, primers, water, and GoTaq®Green Master Mix (part number: M7122, Promega Corporation, Wisconsin, USA). PCR products were analyzed on 2% agarose gel with AccuBand™ 100 bp+3K DNA ladder II (part number: DM2400, Smobio Technology, Inc., Taiwan). Gene expressions were quantified using densitometry analysis with ImageJ® software and then normalized by HPRT1.

Histopathological Evaluations

Tissue sections (4 µm thick) were deparaffinized and stained with hematoxylin and eosin (H&E) or Sirius red (SR). The H&E- and SR-stained slides were examined across the entire visual field of the lung tissue using Olympus CX22 light microscope (at least ×100 magnification). The H&E slides were examined at ×400 magnification. A descriptive analysis was performed by comparing representative images from all study groups.

Immunohistochemical Staining of α-SMA

After deparaffinization, the slides were heated in citrate buffer for 15 min, incubated in 3% H_2O_2 in PBS for endogenous peroxidase inhibition, and incubated in blocking solution using rabbit-DAB (Poly-HRP) detection IHC kit (Catalog number: IHC0007; FineTest®, Wuhan, China). The slides were then incubated at 4 °C overnight with an anti-smooth muscle actin-specific antibody (part number: FNab08038, dilution: 1/500; FineTest®, Wuhan, China). Then, the slides were incubated with species-specific secondary antibodies at room temperature for one hour, followed by incubation with a DAB working solution. Hematoxylin was then used for counterstaining. The slides were examined across the entire visual field of the lung tissue using an Olympus CX22 light microscope (at least ×100 magnification). A descriptive analysis was performed by comparing representative images from all study groups.

Statistical Analysis

Data were analyzed using IBM SPSS Statistics for Windows, version 23.0 (IBM Corp, Armonk, NY, United States). The normality of numeric data was analyzed using the Shapiro-Wilk test. One-way analysis of variance (ANOVA) and the Kruskal-Wallis test were used to assess normal and non-normal distribution of data, respectively. When needed, further analysis including the least significant difference (LSD) test for one-way ANOVA or the Dunn-Bonferroni test for the Kruskal-Wallis test were performed. Paired sample *t* test was used to compare pre- and post-CGA BGL. $P<0.05$ was considered statistically significant.

Results

Blood Glucose Levels

Initially, induction of diabetes was confirmed by evaluating BGL on day six after administration of streptozotocin (pre-CGA). The results showed a significant increase in BGL in all DM and CGA groups compared to the control group (DM1: P=0.037, DM2: P=0.002, CGA1: P=0.011, CGA2: P=0.002, CGA3: P=0.007) (table 2).

Table 1: Sequence of primers and corresponding polymerase chain reaction (PCR) conditions

Gene	Primer sequence	PCR conditions
TGF-β1	5'-GACCGCAACAACGCAATCTA-3' (forward) 5'-TTCCGTCTCCTTGGTTCAGC-3' (reverse)	35 cycles at 94 °C for 10 s, 63 °C for 20 s, 72 °C for 60 s, and last extension at 72 °C for 10 min.
CTGF	5'-CGTAGACGGTAAAGCAATGG-3' (forward) 5'-AGTCAAAGAAGCAGCAAACAC-3' (reverse)	35 cycles at 94 °C for 10 s, 53 °C for 20 s, 72 °C for 60 s, and last extension at 72 °C for 10 min.
Collagen-1	5'-CAACCTCAAGAAGTCCCTGC-3' (forward) 5'-AGGTGAATCGACTGTTGCCT-3' (reverse)	35 cycles at 94 °C for 10 s, 54 °C for 20 s, 72 °C for 60 s, and last extension at 72 °C for 10 min.
α-SMA	5'-CCCAGACACCAGGGAGTGAT-3' (forward) 5'-CGTTAGCAAGGTCGGATGCT-3' (reverse)	35 cycles at 94 °C for 10 s, 65 °C for 20 s, 72 °C for 60 s, and last extension at 72 °C for 10 min.
SMAD7	5'-TTCTTCATGGTGTGCGGAGGTC-3' (forward) 5'-GCTCCAGAAGAAGTTGGGAATCTGA-3' (reverse)	35 cycles at 94 °C for 10 s, 53 °C for 20 s, 72 °C for 60 s, and last extension at 72 °C for 10 min.
HPRT1	5'-AGACGTTCTAGTCCTGTGGC-3' (forward) 5'-ATCAAAAGGGACGCAGCAAC-3' (reverse)	35 cycles at 94 °C for 10 s, 51 °C for 20s , 72 °C for 60 s, and last extension at 72 °C for 10 min.

TGF-β1: Transforming growth factor beta 1; CTGF: Connective tissue growth factor; α-SMA: Alpha smooth muscle actin; SMAD7: Suppressor of mothers against decapentaplegic homolog 7; HPRT1: Hypoxanthine-guanine phosphoribosyltransferase 1

Table 2: Average blood glucose levels in pre-and post-treatment with chlorogenic acid (CGA)

Groups	Pre-CGA (day 6)	Post-CGA (euthanasia)	P value
Control	126.8±48.4	199±35.6	0.124
DM1	322.8±49.9*	448.40±101.8**	0.045***
DM2	429.6±184.8*	550.20±80.9**	0.328
CGA1	387.25±216.8*	290.75±34.2$^{\#,\pm}$	0.418
CGA2	457.5±155.4*	331.25±76.3$^{\#,\pm}$	0.328
CGA3	405.5±110.5*	463.83±87.0$^{**,£,\$}$	0.094

Data are expressed as mean±SD. DM1: Diabetes for six weeks; DM2: Diabetes for eight weeks; CGA1: DM2 group treated with CGA 12.5 mg/Kg BW; CGA2: DM2 group treated with CGA 25 mg/Kg BW; CGA3: DM2 group treated with CGA 50 mg/Kg BW. *, **, #, ±, £, $: P values determined using a one-way ANOVA test followed by an LSD test. ***: Pre- and post-CGA P values determined using paired sample *t* test; P<0.05 vs. pre-CGA of controls; *P<0.05 vs. pre-CGA of controls; **P<0.05 vs. post-CGA of controls; $^{\#}$P<0.05 vs. post-CGA of DM1; $^{\pm}$P<0.05 vs. post-CGA of DM2; $^{£}$P<0.05 vs. post-CGA of CGA1; $^{\$}$P<0.05 vs. post-CGA of CGA2; ***P<0.05

The hypoglycemic effect of CGA in all treatment groups was verified using BGL taken immediately before euthanasia (post-CGA) (table 2). All CGA groups had lower BGL than the DM2 group, especially CGA1 (P≤0.001) and CGA2 (P=0.001). BGL in the CGA3 group was also lower than the DM2 group (P=0.092), but not statistically significant.

Pre- and post-CGA BGL were compared to determine the significance of the glucose-lowering effect of CGA. Post-CGA BGL of the control, DM1, and DM2 groups were higher than pre-CGA levels, although not statistically significant (control: P= 0.124, DM1: P=0.045, DM2: P=0.328) (table 2). Therefore, the results showed that the increase in BGL was not due to interventions. In the groups receiving CGA, especially CGA1 and CGA2, post-CGA BGL were lower than the pre-CGA levels, although not statistically significant (CGA1: P=0.418, CGA2: P=0.328). However, the CGA3 group did not show a glucose-lowering effect compared to its pre-CGA levels (P=0.094). Despite the inadequate glucose-lowering effect of CGA, our results suggest that hypoglycemia might not be dose-dependent.

Histopathological Evaluations

Histology of the lungs of DM-induced rats was examined by H&E staining. Lung tissue sections of the control group showed numerous alveoli, visible alveolar sacs, thin alveolar septa, and a minimum number of alveolar macrophages (figure 1). In the DM1 group, tissue sections showed thickening of alveolar septa filled with cellular infiltration, many alveolar macrophages in the lumen or interstitial area loaded with phagocytosed particles, and collapsed or even obliterated alveoli. In addition, scattered interstitial hemorrhage was observed. These results were especially noticeable in the DM2 group, confirming the success of the DM-induced pulmonary fibrosis model. In contrast, the lung structure of the CGA1 group appeared similar to the control group, but we could still observe interstitial hemorrhage and scattered alveolar macrophages. However, the lung structure of the CGA2 and CGA3 groups was similar to those of the DM groups. Based on the histological findings, CGA at a dose of 12.5 mg/Kg BW showed the best antifibrotic effects.

The Expression of Profibrotic and Antifibrotic Factors

As shown in figure 2, diabetes caused an increase in the expression of profibrotic factors within eight weeks, such as TGF-β1 (DM2: 1.33±0.20, P=0.014) and CTGF (0.95±0.09). Treatment with 12.5 mg/Kg BW CGA (1.01±0.10) significantly lowered TGF-β1 mRNA expression in the CGA1 group compared to the DM2 group (P=0.021) and DM1 group (1.33±0.25, P=0.05). This confirms the antifibrotic effect of CGA. Treatment with 25 and 50 mg/Kg BW CGA increased TGF-β1 mRNA expression in the CGA2 and CGA3 groups by more than 1.5- and two-fold (1.47±0.14, P=0.014 and 1.89±0.51, P=0.01; respectively) compared to the control group (0.92±0.34). There was no significant difference in CTGF mRNA expression between the groups (figure 2B). However, the expressions were generally lower in the CGA groups (CGA1: 0.60±0.24, CGA2: 0.76±0.09, CGA3: 0.52±0.49) than the DM groups (DM1: 0.78±0.18, DM2: 0.95±0.09). The SMAD7 (suppressor of mothers against decapentaplegic 7) expression was lower in the DM groups than the control group (DM1: 0.72±0.15, P=0.33; DM2: 0.58±0.11, P=0.13). Moreover, the expression was higher in the CGA groups, especially in the CGA1 group (CGA1: 1.04±0.27, CGA2: 0.78±0.16, CGA3: 0.93±0.28) than both DM1 (CGA1: P=0.13, CGA2: P=0.74, CGA3: P=0.62) and DM2 (CGA1: P=0.04, CGA2: P=0.76, CGA3: P=0.26) groups (figure 2C).

Myofibroblasts Transformation and Collagen Synthesis

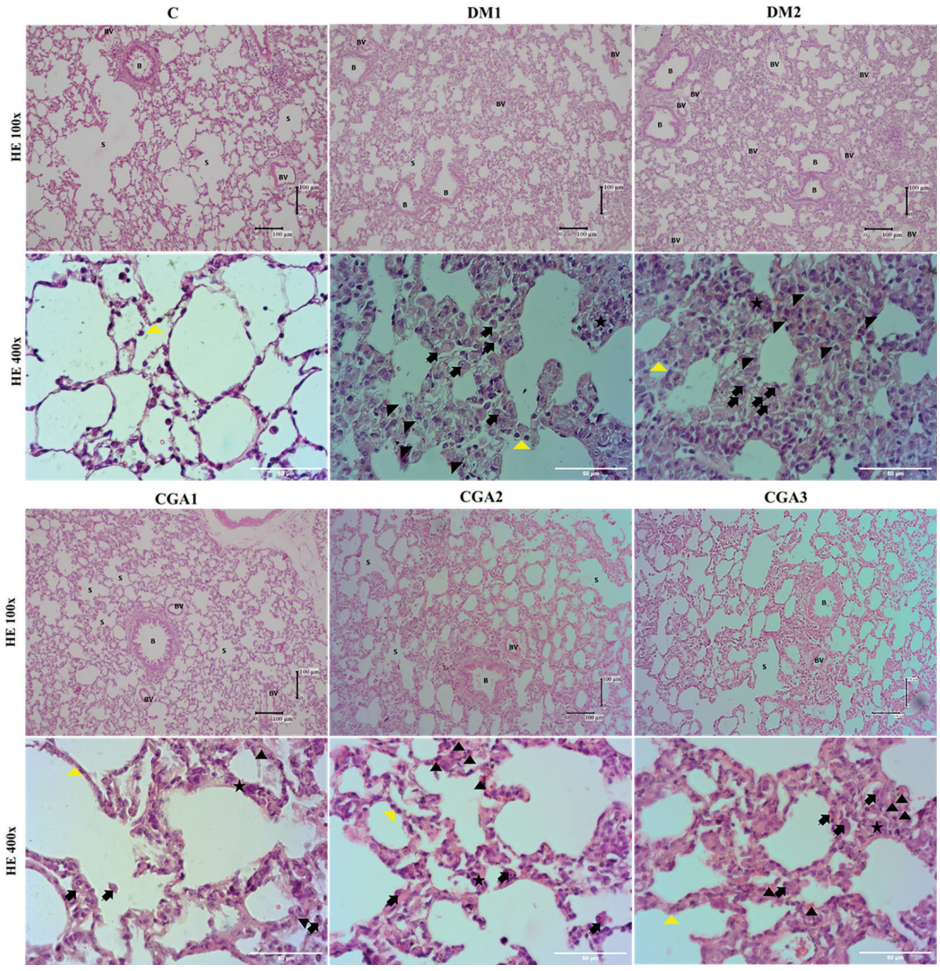

Figure 1: A magnified view of the lung structure stained with hematoxylin-eosin (×100 and ×400 magnification with 100 µm and 50 µm scale bar, respectively). Yellow triangles show interalveolar septa (notice the difference in thickness between groups). Stars show thickening of interalveolar septa filled with inflammatory cells (notice collapsed or obliterated alveoli in the DM1, DM2, CGA2, and CGA3 groups). Black triangles represent interstitial hemorrhage. Arrows show alveolar macrophages in the interstitial and alveolar lumen. B: Bronchioles; BV: Blood vessels; S: Alveolar sacs.

The results showed no significant difference in the α-SMA mRNA expression (a marker of myofibroblast transformation) between the groups (P=0.199). However, there was an increase in the expression of α-SMA in DM groups compared to the control group (DM1: median 0.44, interquartile range [IQR] 0.42-0.80; DM2: median 0.76, IQR 0.66-1.10) (figure 3A). These were similar to the results of immunohistochemical staining that showed a higher expression of α-SMA in the peribronchiolar and perivascular regions of DM1 and DM2 groups than the control group (figure 3C). After treatment with CGA, a reduction in the expression of α-SMA was found in the CGA1 (median 0.60, IQR 0.34-0.64) and CGA2 (median 0.53, IQR 0.41-0.64) groups compared to DM1 and DM2. However, α-SMA mRNA expression was slightly increased in the CGA3 group (median 1.06, IQR 0.46-1.23) compared to the DM2 group.

The expression of collagen-1 in the DM groups (DM1: 0.96±0.21, P=0.10; DM2: 1.16±0.10, P=0.11) were higher than the control group (0.65±0.10) (figure 3A). Deposition of collagen fiber in the peribronchiolar region and thickening of the interalveolar septum were observed in the DM groups (figure 3C). The results of RT-PCR showed a lower expression of collagen-1 in the CGA1 group (0.75±0.13) than the DM groups (DM1: P=0.24, DM2: P=0.26). The lung structure of the CGA1 group was also similar to the control group, but the interalveolar septum was thicker (figure 3C). The expression of collagen-1 in the CGA3 group (1.24±0.31) was higher than the DM groups (DM1: P=0.13; DM2: P=0.12), and even the CGA1 group (P=0.01) (figure 3A). In the CGA3 group, significant deposition of collagen fiber in the peribronchiolar and perivascular regions and thickening of interalveolar septal were observed (figure 3C). This indicates that the effect of CGA in lowering BGL and reducing lung fibrosis might not be dose-dependent. However, treatment with 12.5 mg/Kg BW CGA was slightly more effective than in higher doses.

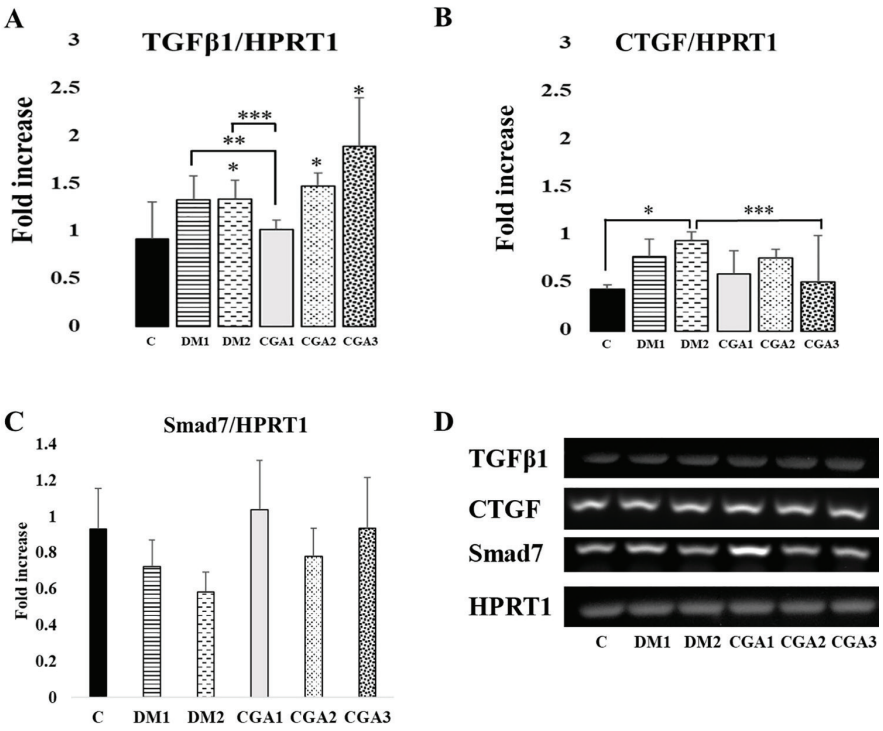

Figure 2: Comparison between the mRNA expression of TGF-β1 and CTGF (profibrotic factors) and SMAD7 (antifibrotic factor) between the groups. P values were determined using a one-way ANOVA test. (A, B) Significant differences were found in the mRNA expression of TGF-β1 between the CGA1 group and DM groups, but no significant difference was observed in the mRNA expression of CTGF between the groups. (C) A significant difference was observed in the mRNA expression of SMAD7 between the CGA1 and DM2 groups. (D) Results of electrophoresis for the mRNA expressions of TGF-β1, CTGF, and SMAD7. TGF-β1: Transforming growth factor beta 1; CTGF: Connective tissue growth factors; HPRT1: Hypoxanthine phosphoribosyl transferase 1; SMAD7: Suppressor of mothers against decapentaplegic 7; *P<0.05 vs. control; **P<0.05 vs. DM1; ***P<0.05 vs. DM2

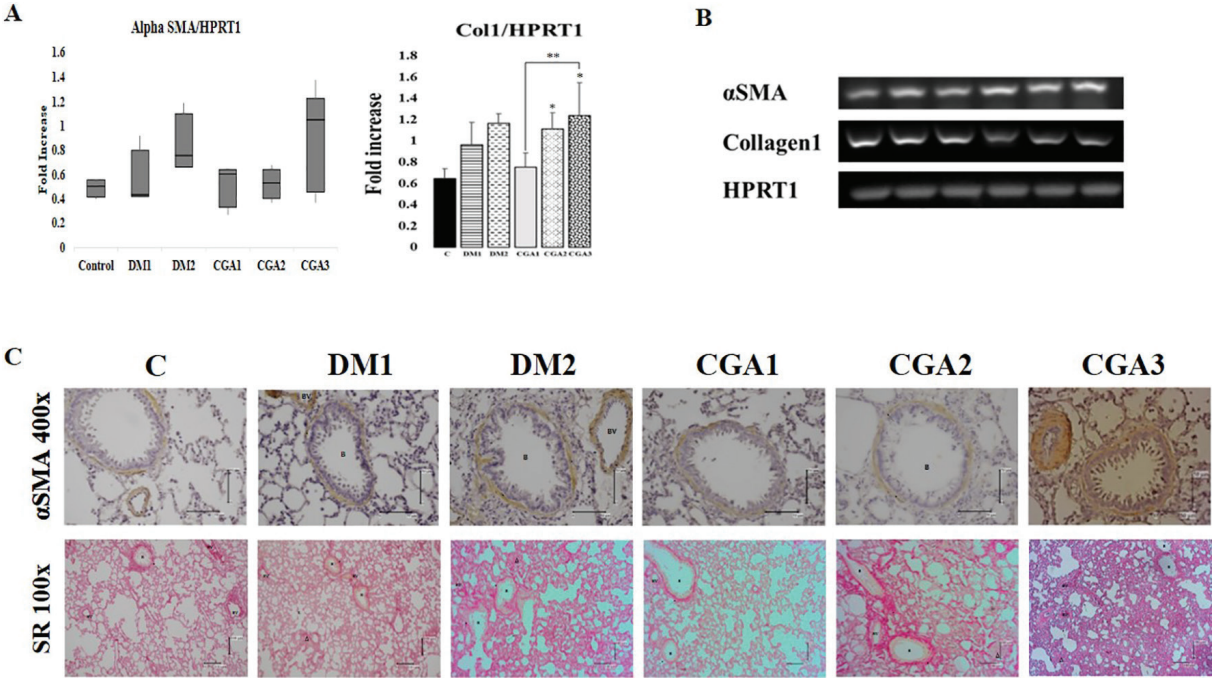

Figure 3: A comparison between the mRNA expression of α-SMA and collagen-1 between the groups. (A) α-SMA data are presented in box plots and expressed as median with IQR. P values are determined using the Kruskal-Wallis test. No significant difference was observed in the mRNA expression of α-SMA between the groups. Collagen-1 data are obtained using one-way ANOVA and expressed as mean±SD. (*P<0.05 vs. control, **P<0.05 vs. CGA1). (B) Results of electrophoresis for the mRNA expressions of α-SMA and collagen-1. (C) A magnified view of the lung structure after immunohistochemical staining of α-SMA and Sirius red staining (×400 and ×100 magnification with 50 μm and 100 μm scale bar, respectively). Black triangles represent the deposition of collagen fiber. B: Bronchioles; BV: Blood vessels; S: Alveolar sacs; α-SMA: Alpha-smooth muscle actin.

Discussion

Diabetes was induced by a single-dose of streptozotocin to cause pulmonary fibrosis in rats. Six days after the induction, compared to controls, a uniform increase in BGL was observed. In line with a previous study,[20] histological analyses showed that diabetes was successfully induced after six and eight weeks. The results showed thickened alveolar septa filled with cellular infiltration and the collapse of some air sacs, while some others were dilated. We also observed attenuation of the epithelial lining of the bronchioles in certain areas, as well as pulmonary congestion of blood vessels with thickened walls. The expression of fibrotic (TGF-β1, CTGF, α-SMA, collagen 1) and antifibrotic (SMAD7) factors were evaluated. There was a consistent increase in the expression of profibrotic factors and a decrease in the antifibrotic factor in the DM groups, whose effect was time-dependent.

Based on BGL, a similar hypoglycemic effect of CGA, especially at doses of 12.5 and 25 mg/Kg BW, in all treatment groups compared to controls was confirmed. However, treatment with 50 mg/Kg BW CGA showed lower BGL, but the difference compared to other doses was not statistically significant. To the best of our knowledge, for the first time, we found that the hypoglycemic effect of CGA might not be dose-dependent. In the case of type 1 diabetes, these findings demonstrated the role of CGA in lowering BGL by increasing insulin secretion from active pancreatic beta cells. These results are supported by an *in vitro* study using an INS-1E cell line, reporting that CGA in a dose of 50 g/mL (equivalent to the effect of 5 mM glucose) increased insulin secretion.[21]

To further evaluate the role of CGA in lowering BGL, we compared pre- and post-CGA glucose levels. The results showed that BGL increased in the control and DM groups, while it decreased in the CGA1 and CGA2 groups, though the difference was not statistically significant. Moreover, the increase in the CGA3 group was not statistically significant. These results may indicate the lack of hypoglycemic effect of CGA at a dose of 50 mg/Kg BW. In contrast, Bagdas and others showed that the administration of CGA at a dose of 50 mg/Kg BW for 15 days significantly decreased BGL.[22] The difference in results could be attributed to the timing and dose of CGA administration. In another study, Bagdas and others reported no hypoglycemic effect after seven days of CGA administration at a dose of 100 mg/Kg BW.[23] As mentioned earlier, increasing insulin secretion is one of the hypoglycemic mechanisms of CGA.[21] This may be related to the effect of stress on vital organs due to long-term drug use[22, 23] that might further damage pancreatic cells.[24]

Histological features of the CGA-treated groups were also evaluated. The results showed that lung tissue repair was similar in both the CGA1 and control groups. However, fibrosis was still observed in the CGA2 and CGA3 groups. These results were consistent with the mRNA expression of the TGF-β1 gene as the main profibrotic factor. TGF-β1 mRNA expression was the lowest in the CGA1 group, while the expression in the CGA2 and CGA3 groups was higher than in the DM groups. The effect of CGA on reducing TGF-β1 expression can be influenced by the effect of hypoglycemia or directly due to the inhibition of endoplasmic reticulum stress. A previous study demonstrated the proliferation of RLE-6TN cells induced by TGF-β1. Furthermore, CGA administration could significantly inhibit the expression of GRP78 (glucose-regulated protein-78), downregulate the level of phosphorylation of PERK (PKR-like endoplasmic reticulum kinase), and activate AFT-6 (activating transcription factor 6).[18] Hypoglycemia can also reduce the expression of TGF-β1 by decreasing inflammatory mediators. In hyperglycemia, activation of NF-κB due to oxidative stress causes an increase in genes encoding proinflammatory cytokines such as tumor necrosing factor alpha (TNF-α), monocyte chemotactic protein-1 (MCP1), and several other chemokines; leading to the accumulation of inflammatory cells and activation of macrophages.[7] Activated macrophages secrete TGF-β1, as the most potent profibrotic factor, and activate monocytes and fibroblasts through fibroblast growth factor-2 (FGF-2) and the mitogen-activated protein kinase (MAPK) pathway, resulting in the induction of fibrosis.[7, 9, 25]

The expression of TGF-β1 mRNA in the CGA2 and CGA3 groups may be related to the prooxidative state due to the dose of CGA. A follow-up study by Bagdas and others on the adverse effects of CGA showed that CGA at a dose of ≥50 mg for a prolonged period could cause a genotoxic effect due to prooxidants, as evidenced by increased micronuclei formation. The prooxidant effect is enhanced in the liver, kidney, and bone marrow.[26] Some studies showed that high doses of certain phenolic compounds (e.g., kaempferol, caffeic acid, quercetin, and ferulic acid) can cause genotoxic and prooxidant effects, especially in the presence of metal ions.[27-33] Phenolic compounds can exhibit prooxidant effects, especially in systems containing iron or copper, to catalyze

redox cycles and form phenolic radicals which damage lipids and DNA.[34] Another characteristic of fibrosis, namely alveolar collapse as observed in the histological results of the CGA2 and CGA3 groups in our study, may be due to the release of free radicals by leukocytes in the inflamed area, causing an increase in lipid peroxidase which hydrolyzes surfactant lipids, and in turn a decrease in alveolar surface tension.[20] High levels of lipid peroxidase were reported with the administration of CGA at a dose of 100 mg/ Kg BW in the liver and kidneys.[26] However, the association of these genotoxic and cytotoxic effects with increasing BGL is not yet known.

The expression of CTGF, another profibrotic agent that acts as a cofactor of TGF-β1 in fibroblasts, was also evaluated. CTGF plays a role in the transcriptional activation of COL1A2 and α-SMA expression in myofibroblast formation.[35] A decrease in CTGF mRNA expression in the treatment groups was observed, but the decrease was not statistically significant compared to DM groups. CTGF itself is activated by TGF-β1 and plays a role in the production, adhesion, and contraction of the extracellular matrix by acting as a pro-adhesive molecule of integrins and proteoglycans.[35] In pulmonary fibrosis, however, inhibition of CTGF can prevent and reverse the fibrosis process through the mechanism of anti-CTGF monoclonal antibody FG-3019.[36] In line with the results of a previous study, we found a decrease in CTGF mRNA expression in the CGA groups.[37] Qin and others reported that CGA administration could inhibit the expression of CTGF and fibronectin as one of the effector molecules in the mechanism of cardiac fibrosis. CGA activates the cyclic GMP/ protein kinase G (cGMP/PKG) pathway to block nuclear translocation of P-SMAD2/3 induced by hyperglycemia, thereby reducing the expression of fibrosis-related genes in cardiac fibroblasts without relying on the cardiac hypoglycemic mechanism of CGA.[37]

A previous study showed that elevated levels of SMAD7 partially protect the lungs during the initial stages of diabetes by inhibiting SMAD-dependent TGFβ1 gene activation in a diabetic rat model. Therefore, elevated SMAD7 levels might delay the onset of fibrosis in the lungs when other organs such as kidneys and liver are already affecteded.[7] Our results showed lower SMAD7 mRNA expression in the DM2 group than the DM1 group. Moreover, CGA-treated groups exhibited higher SMAD7 mRNA expression than DM groups, especially the lower CGA dose group. Studies on liver fibrosis have shown the beneficial effect of CGA in promoting SMAD7 mRNA and protein levels in a model of CCl4-induced liver fibrosis and *Schistosoma japonicum* cercaria.[38, 39] However, we found no other studies on the effect of CGA in promoting SMAD7 expression in the lungs of animal models of diabetes.

In the present study, we also demonstrated the role of CGA in reducing mRNA expression in fibrosis-related genes (collagen-1 and α-SMA), especially in the CGA1 group. Histological image analysis of the H&E-stained lungs of DM groups, CGA2, and CGA3 showed thickening of the interalveolar septum filled with proinflammatory cells and profibrotic factors, whereas the CGA1 group showed a thinner interalveolar septum. These results were verified by SR staining that showed the tissue structure of the CGA1 group was similar to the control group with less deposition of collagen. In addition, immunohistochemical staining showed reduced α-SMA expression compared to the DM, CGA2, and CGA3 groups; where TGF-β1 mainly affected the modulation of the main profibrotic factors collagen-1 and α-SMA.[35, 40] The decrease in these factors may be caused by the downstream mechanism of the TGF-β1 pathway or directly due to the expression of collagen-1 and α-SMA. The role of CGA in inhibiting the expression of collagen-1 and α-SMA were reported in rat liver fibrosis induced by carbon tetrachloride.[16]

As a limitation of our study, we did not evaluate the exact CGA mechanism of inflammatory and oxidation pathways in the lungs.

Conclusion

The role of CGA in inhibiting diabetes-induced progressive pulmonary fibrosis were demonstrated. CGA at a dose of 12.5 mg/ Kg BW reduced the expression of profibrotic factors and increased antifibrotic factors in rats. The results of H&E staining showed that lung tissue structure at the low-dose CGA was similar to the control group, with less deposition of collagen (SR staining), and reduced expression of myofibroblasts. Our findings provide a better understanding of the effect of low-dose CGA on hypoglycemia and fibrosis in diabetes complications.

Acknowledgment

The present manuscript is submitted in partial fulfillment of the requirements for the Master's degree of S.M.S Kencana. The study was financially supported by the "Penelitian Tesis Magister" of the Indonesian Government (2022). Technical assistance by Mr. Mulyana is greatly appreciated.

Authors' Contribution

SMS.K, N.A, R.Y: Data analysis and interpretation; SMS.K, RLAW.S, F.M: Draft version of the manuscript; N.A, R.Y, DCR.S: Revising the manuscript. All authors have contributed to the study design and approved the final version of the manuscript. They agree to be accountable for all aspects of the work in ensuring that questions related to the accuracy or integrity of any part of the work are appropriately investigated and resolved.

Conflict of Interest: None declared.

References

1 Magliano DJ, Boyko EJ. IDF Diabetes Atlas. 10th ed. Brussels: International Diabetes Federation; 2021.

2 da Silva Almeida R, de Melo RC, Chaves MSS, Baptista GM, Margotto SS, de Oliveira Andrade LJ. Diabetic pneumopathy. Brazilian Journal of Medicine and Human Health (inactive/archive only). 2016;4. doi: 10.17267/2317-3386bjmhh.v4i1.791.

3 Rajasurya V, Gunasekaran K, Surani S. Interstitial lung disease and diabetes. World J Diabetes. 2020;11:351-7. doi: 10.4239/wjd.v11.i8.351. PubMed PMID: 32864047; PubMed Central PMCID: PMCPMC7438183.

4 Wang D, Ma Y, Tong X, Zhang Y, Fan H. Diabetes Mellitus Contributes to Idiopathic Pulmonary Fibrosis: A Review From Clinical Appearance to Possible Pathogenesis. Front Public Health. 2020;8:196. doi: 10.3389/fpubh.2020.00196. PubMed PMID: 32582606; PubMed Central PMCID: PMCPMC7285959.

5 Hamdy G, Amin M, Rashad A. Pulmonary function changes in diabetic lung. Egyptian Journal of Chest Diseases and Tuberculosis. 2013;62:513-7. doi: 10.1016/j.ejcdt.2013.07.006.

6 Schuyler MR, Niewoehner DE, Inkley SR, Kohn R. Abnormal lung elasticity in juvenile diabetes mellitus. Am Rev Respir Dis. 1976;113:37-41. doi: 10.1164/arrd.1976.113.1.37. PubMed PMID: 1247213.

7 Talakatta G, Sarikhani M, Muhamed J, Dhanya K, Somashekar BS, Mahesh PA, et al. Diabetes induces fibrotic changes in the lung through the activation of TGF-beta signaling pathways. Sci Rep. 2018;8:11920. doi: 10.1038/s41598-018-30449-y. PubMed PMID: 30093732; PubMed Central PMCID: PMCPMC6085305.

8 Bai L, Zhang L, Pan T, Wang W, Wang D, Turner C, et al. Idiopathic pulmonary fibrosis and diabetes mellitus: a meta-analysis and systematic review. Respir Res. 2021;22:175. doi: 10.1186/s12931-021-01760-6. PubMed PMID: 34103046; PubMed Central PMCID: PMCPMC8188656.

9 Rout-Pitt N, Farrow N, Parsons D, Donnelley M. Epithelial mesenchymal transition (EMT): a universal process in lung diseases with implications for cystic fibrosis pathophysiology. Respir Res. 2018;19:136. doi: 10.1186/s12931-018-0834-8. PubMed PMID: 30021582; PubMed Central PMCID: PMCPMC6052671.

10 Wuyts WA, Agostini C, Antoniou KM, Bouros D, Chambers RC, Cottin V, et al. The pathogenesis of pulmonary fibrosis: a moving target. Eur Respir J. 2013;41:1207-18. doi: 10.1183/09031936.00073012. PubMed PMID: 23100500.

11 Nicholas SB. Novel Anti-inflammatory and Anti-fibrotic Agents for Diabetic Kidney Disease-From Bench to Bedside. Adv Chronic Kidney Dis. 2021;28:378-90. doi: 10.1053/j.ackd.2021.09.010. PubMed PMID: 34922694.

12 Mummidi S, Das NA, Carpenter AJ, Kandikattu H, Krenz M, Siebenlist U, et al. Metformin inhibits aldosterone-induced cardiac fibroblast activation, migration and proliferation in vitro, and reverses aldosterone+salt-induced cardiac fibrosis in vivo. J Mol Cell Cardiol. 2016;98:95-102. doi: 10.1016/j.yjmcc.2016.07.006. PubMed PMID: 27423273.

13 Rangarajan S, Bone NB, Zmijewska AA, Jiang S, Park DW, Bernard K, et al. Metformin reverses established lung fibrosis in a bleomycin model. Nat Med. 2018;24:1121-7. doi: 10.1038/s41591-018-0087-6. PubMed PMID: 29967351; PubMed Central PMCID: PMCPMC6081262.

14 Liang N, Kitts DD. Role of Chlorogenic Acids in Controlling Oxidative and Inflammatory Stress Conditions. Nutrients. 2015;8. doi: 10.3390/nu8010016. PubMed PMID: 26712785; PubMed Central PMCID: PMCPMC4728630.

15 Ong KW, Hsu A, Tan BK. Anti-diabetic and anti-lipidemic effects of chlorogenic acid are mediated by ampk activation. Biochem Pharmacol. 2013;85:1341-51. doi: 10.1016/j.bcp.2013.02.008. PubMed PMID: 23416115.

16 Shi H, Dong L, Jiang J, Zhao J, Zhao G, Dang X, et al. Chlorogenic acid reduces liver inflammation and fibrosis through inhibition of toll-like receptor 4 signaling pathway.

Toxicology. 2013;303:107-14. doi: 10.1016/j.tox.2012.10.025. PubMed PMID: 23146752.
17 Yunus J, Salman M, Lintin GBR, Muchtar M, Sari DCR, Arfian N, et al. Chlorogenic acid attenuates kidney fibrosis via antifibrotic action of BMP-7 and HGF. Med J Malaysia. 2020;75:5-9. PubMed PMID: 32471962.
18 Wang YC, Dong J, Nie J, Zhu JX, Wang H, Chen Q, et al. Amelioration of bleomycin-induced pulmonary fibrosis by chlorogenic acid through endoplasmic reticulum stress inhibition. Apoptosis. 2017;22:1147-56. doi: 10.1007/s10495-017-1393-z. PubMed PMID: 28677092.
19 Kilkenny C, Browne WJ, Cuthill IC, Emerson M, Altman DG. Improving bioscience research reporting: the ARRIVE guidelines for reporting animal research. PLoS Biol. 2010;8:e1000412. doi: 10.1371/journal.pbio.1000412. PubMed PMID: 20613859; PubMed Central PMCID: PMCPMC2893951.
20 Soliman ME. Evaluation of Time Dependent Changes of the Rat's Lung in Experimentally Induced Diabetes Mellitus: Light and Electron Microscopic Study. Egyptian Journal of Histology. 2010;33:45-54. doi: 10.1097/00767537-201003000-00006.
21 Alam S, Sarker MMR, Sultana TN, Chowdhury MNR, Rashid MA, Chaity NI, et al. Antidiabetic Phytochemicals From Medicinal Plants: Prospective Candidates for New Drug Discovery and Development. Front Endocrinol (Lausanne). 2022;13:800714. doi: 10.3389/fendo.2022.800714. PubMed PMID: 35282429; PubMed Central PMCID: PMCPMC8907382.
22 Bagdas D, Etoz BC, Gul Z, Ziyanok S, Inan S, Turacozen O, et al. In vivo systemic chlorogenic acid therapy under diabetic conditions: Wound healing effects and cytotoxicity/genotoxicity profile. Food Chem Toxicol. 2015;81:54-61. doi: 10.1016/j.fct.2015.04.001. PubMed PMID: 25846499.
23 Bagdas D, Cam Etoz B, Inan Ozturkoglu S, Cinkilic N, Ozyigit MO, Gul Z, et al. Effects of systemic chlorogenic acid on random-pattern dorsal skin flap survival in diabetic rats. Biol Pharm Bull. 2014;37:361-70. doi: 10.1248/bpb.b13-00635. PubMed PMID: 24389556.
24 Eizirik DL, Pasquali L, Cnop M. Pancreatic beta-cells in type 1 and type 2 diabetes mellitus: different pathways to failure. Nat Rev Endocrinol. 2020;16:349-62. doi: 10.1038/s41574-020-0355-7. PubMed PMID: 32398822.
25 Saito A, Horie M, Nagase T. TGF-beta Signaling in Lung Health and Disease. Int J Mol Sci. 2018;19. doi: 10.3390/ijms19082460. PubMed PMID: 30127261; PubMed Central PMCID: PMCPMC6121238.
26 Bagdas D, Gul NY, Topal A, Tas S, Ozyigit MO, Cinkilic N, et al. Pharmacologic overview of systemic chlorogenic acid therapy on experimental wound healing. Naunyn Schmiedebergs Arch Pharmacol. 2014;387:1101-16. doi: 10.1007/s00210-014-1034-9. PubMed PMID: 25129377.
27 Chu KO, Chan SO, Pang CP, Wang CC. Pro-oxidative and antioxidative controls and signaling modification of polyphenolic phytochemicals: contribution to health promotion and disease prevention? J Agric Food Chem. 2014;62:4026-38. doi: 10.1021/jf500080z. PubMed PMID: 24779775.
28 Leon-Gonzalez AJ, Auger C, Schini-Kerth VB. Pro-oxidant activity of polyphenols and its implication on cancer chemoprevention and chemotherapy. Biochem Pharmacol. 2015;98:371-80. doi: 10.1016/j.bcp.2015.07.017. PubMed PMID: 26206193.
29 Maurya DK, Devasagayam TP. Antioxidant and prooxidant nature of hydroxycinnamic acid derivatives ferulic and caffeic acids. Food Chem Toxicol. 2010;48:3369-73. doi: 10.1016/j.fct.2010.09.006. PubMed PMID: 20837085.
30 Murakami A. Dose-dependent functionality and toxicity of green tea polyphenols in experimental rodents. Arch Biochem Biophys. 2014;557:3-10. doi: 10.1016/j.abb.2014.04.018. PubMed PMID: 24814373.
31 Robaszkiewicz A, Balcerczyk A, Bartosz G. Antioxidative and prooxidative effects of quercetin on A549 cells. Cell Biol Int. 2007;31:1245-50. doi: 10.1016/j.cellbi.2007.04.009. PubMed PMID: 17583542.
32 Suh KS, Chon S, Oh S, Kim SW, Kim JW, Kim YS, et al. Prooxidative effects of green tea polyphenol (-)-epigallocatechin-3-gallate on the HIT-T15 pancreatic beta cell line. Cell Biol Toxicol. 2010;26:189-99. doi: 10.1007/s10565-009-9137-7. PubMed PMID: 19757103.
33 Upadhyay S, Dixit M. Role of Polyphenols and Other Phytochemicals on Molecular Signaling. Oxid Med Cell Longev. 2015;2015:504253. doi: 10.1155/2015/504253. PubMed PMID: 26180591; PubMed Central PMCID: PMCPMC4477245.
34 Sotler R, Poljsak B, Dahmane R, Jukic T, Pavan Jukic D, Rotim C, et al. Prooxidant Activities of Antioxidants and Their Impact on Health. Acta Clin Croat. 2019;58:726-36. doi: 10.20471/acc.2019.58.04.20. PubMed PMID: 32595258; PubMed Central PMCID:

PMCPMC7314298.
35 Tam AYY, Horwell AL, Trinder SL, Khan K, Xu S, Ong V, et al. Selective deletion of connective tissue growth factor attenuates experimentally-induced pulmonary fibrosis and pulmonary arterial hypertension. Int J Biochem Cell Biol. 2021;134:105961. doi: 10.1016/j.biocel.2021.105961. PubMed PMID: 33662577; PubMed Central PMCID: PMCPMC8111417.
36 Lipson KE, Wong C, Teng Y, Spong S. CTGF is a central mediator of tissue remodeling and fibrosis and its inhibition can reverse the process of fibrosis. Fibrogenesis Tissue Repair. 2012;5:S24. doi: 10.1186/1755-1536-5-S1-S24. PubMed PMID: 23259531; PubMed Central PMCID: PMCPMC3368796.
37 Qin L, Zang M, Xu Y, Zhao R, Wang Y, Mi Y, et al. Chlorogenic Acid Alleviates Hyperglycemia-Induced Cardiac Fibrosis through Activation of the NO/cGMP/PKG Pathway in Cardiac Fibroblasts. Mol Nutr Food Res. 2021;65:e2000810. doi: 10.1002/mnfr.202000810. PubMed PMID: 33200558.
38 Wang Y, Yang F, Xue J, Zhou X, Luo L, Ma Q, et al. Antischistosomiasis Liver Fibrosis Effects of Chlorogenic Acid through IL-13/miR-21/Smad7 Signaling Interactions In Vivo and In Vitro. Antimicrob Agents Chemother. 2017;61. doi: 10.1128/AAC.01347-16. PubMed PMID: 27872076; PubMed Central PMCID: PMCPMC5278737.
39 Yang F, Luo L, Zhu ZD, Zhou X, Wang Y, Xue J, et al. Chlorogenic Acid Inhibits Liver Fibrosis by Blocking the miR-21-Regulated TGF-beta1/Smad7 Signaling Pathway in Vitro and in Vivo. Front Pharmacol. 2017;8:929. doi: 10.3389/fphar.2017.00929. PubMed PMID: 29311932; PubMed Central PMCID: PMCPMC5742161.
40 Hillege MMG, Galli Caro RA, Offringa C, de Wit GMJ, Jaspers RT, Hoogaars WMH. TGF-beta Regulates Collagen Type I Expression in Myoblasts and Myotubes via Transient Ctgf and Fgf-2 Expression. Cells. 2020;9. doi: 10.3390/cells9020375. PubMed PMID: 32041253; PubMed Central PMCID: PMCPMC7072622.